

---

---

**CHAPTER 1**

---

---

# Atomic Force Microscopy in Cancer Cell Research

**Igor Sokolov***Department of Physics and Chemistry, Clarkson University, Potsdam, NY 13699, USA***CONTENTS**

1. Introduction . . . . .	1
1.1. Principles of AFM . . . . .	2
1.2. Modes of AFM Operation . . . . .	2
1.3. Advantages of AFM in Biology . . . . .	4
2. AFM in Study of Cancer Cells: General Overview . . . . .	5
2.1. AFM Detection of Surface Interactions (Atomic Force Spectroscopy) . . . . .	5
2.2. Cellular Sound (Sonocytology) . . . . .	5
2.3. Cell Mechanics . . . . .	6
3. AFM in Study Mechanics of Cancer Cells: Details . . . . .	6
3.1. Rigidity of Cells: Where we are in Numbers . . . . .	6
3.2. How to Measure Rigidity of Cells with AFM: Experimental Steps . . . . .	7
3.3. How to Measure Cell Rigidity with AFM: Young's Modulus Calculations . . . . .	9
3.4. Mechanics of Cancer Cells: Results . . . . .	10
3.5. Discussion . . . . .	12
4. Conclusions and Future Directions . . . . .	14
References . . . . .	15

**1. INTRODUCTION**

There is no need to describe the importance of studying the problem of cancer. Atomic force microscopy (AFM) is a novel technique, arising out of and a form of scanning probe microscopy (SPM), and which is one of the (if not the) major technique responsible for the emergence of modern nanotechnology. AFM has great potential in biology, in particular, to study cells [1–49]. Therefore it is natural to try to understand what is done and what can be done with this technique to study cancer cells. This paper reviews the existing results of the study of cancer cells with AFM. The main focus is made on studying the mechanics of cancer cells; in particular, in comparison with those of normal cells.

Although there are not many results as yet, it would be useful to present what we do know it in a systematic way, to summarize and to discuss future directions.

Because AFM technique, in particular, the part of it that deals with force measurements, is still not very familiar to the broad community of scientists, we start from a brief description of the main principles of AFM. Then, we highlight the main advantages of using AFM in biology. After this introduction, we will overview the main applications in AFM in the study of cancer cells. The study of the mechanics of cancer cells, presumably one of the most promising areas of research, will be analyzed and discussed in detail. The necessity of such a detailed overview of AFM procedure is dictated by both the complexity of this technique and the

present state of research in this area. There are many different interesting results but without a unifying protocol. One of the purposes of this review is to help develop such a protocol.

### 1.1. Principles of AFM

AFM is a relatively novel method. It was invented in 1986 as the first new extension of scanning probe microscopy (which first appeared in 1981 in the guise of scanning tunneling microscopy) [50]. Its technique is based on detection of forces acting between a sharp probe, known as AFM tip, and the sample's surface (Fig. 1). The tip is attached to a very flexible cantilever. Any motion of the cantilever is detected by various methods. The most popular is an optical system of detection. Laser light is reflected from the cantilever and detected by a photodiode. The tip is brought to contact or near-contact with the surface of interest. Scanning over the surface, AFM system records the deflection of the cantilever, due to very small forces between the atoms of the probe and the surface, with sub-nanometer precision. In principle, the whole system may look like just an old-fashioned stylus profilometer. Indeed, the only difference is the presence in AFM of a very sensitive detection system, microscopically sharp tips, and extremely high-precision tip-sample positioning. The deflection signal (or any derivations of the deflection) is recorded digitally, and can be visualized on a computer in real-time.

The AFM technique is much more than just simply microscopy. One can think about AFM tip as a microscopic "finger" with a nanosize apex. Following this analogy, one can use such a finger to touch the surface to feel how rigid it is (rigidity force microscope or nanoindenter); one can feel how sticky a surface is (chemical force microscopy); one can put some "goo" on the top of the tip, and consequently, detect how sticky the "goo" is with respect to the surface (functionalized tip imaging); and so on. In essence, one can do with AFM correspondingly what can be done with "a learning finger." Depending on the sample and on information that one wishes to get, one can choose many different *modes of operation* of AFM.

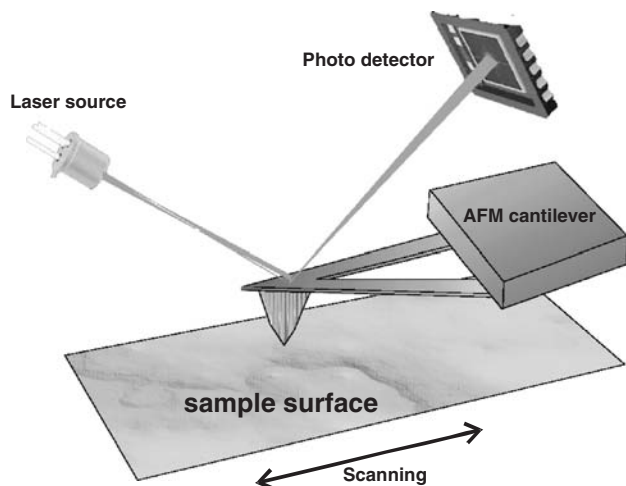


Figure 1. A schematic view of the AFM method.

### 1.2. Modes of AFM Operation

Here we briefly describe a few basic modes which one can operate an AFM in: contact, tapping, and force mode. There are a few other modes of operation, which are not that popular as yet, and will not be described here. An advanced, so-called force-volume mode, which is rather useful for the study cell mechanics, will also be presented. All modes work in ambient conditions, as well as in liquids, including biological buffers. Comparative advantages and disadvantages of these modes are also described below.

#### 1.2.1. Contact Mode

In contact mode, AFM tip is in actual contact with the sample's surface. In principle, AFM in this mode can work precisely as described above. However, if there is a bump on the surface, the cantilever will be deflected more, and consequently, AFM tip scans over the surface with more force. This can result in scratching the sample surface. Moreover, if the sample surface has a trench, the cantilever may simply "fly over" without touching it. Both cases are not good. To exclude these bad behaviors of the cantilever, a positive-feedback system was introduced. This works as follows. When the tip comes across a bump on the surface, the deflection of the cantilever increases, and the feedback system elevates the whole cantilever holder so that the cantilever's deflection is adjusted back to its original value, and the cantilever is returned to its original position. In the case of a trench, the same feedback system moves the cantilever down to again, maintain the same deflection. This provides the same so-called "load force" between the tip and the sample.

Pros of contact mode:

- This is the simplest mode of operation. It requires minimum operational skill and only basic hardware.
- Allows very fast scanning (typically 0.1–0.5 second per scan line).
- The load force can be precisely controlled.
- Good signal-to-noise ratio even in a noisy environment.
- Generally cheaper and more robust cantilevers can be used.

Cons of contact mode:

- The tip can stretch or even scratch the surface. This will lead to artifacts, therefore disrupting the sample and leading to images and measurements that are not representational of the original sample.
- The tip can remove poorly attached parts of the sample. Apart from just damaging the surface, this can contaminate the tip surface and prevent it from being used any further.
- Can provide only limited information about the surface (comparing to other modes).

Because of its simplicity, contact mode is one of the most popular modes. Contact mode is typically the best on solid and well-fixed surfaces. It normally requires rather soft cantilevers (spring constant (a characteristic measure) in the range of 0.001–1  $\text{Nm}^{-1}$ ).

### 1.2.2. Tapping/AC/Intermittent Contact Mode

To further minimize the tip impact onto the surface, *dynamic* or *intermittent contact mode*, also commonly known as *Tapping mode* (a trademark of Veeco Instruments, Inc.), was introduced. Another name use for this mode is AC mode. In this mode the tip “taps,” or oscillates up and down very fast, touching the sample surface for a very short period of time during relatively slow lateral scanning. This considerably decreases scratching (although it does not eliminate it completely). While in contact mode cantilever deflection is detected and measured, in this mode the amplitude of oscillation is typically measured. Positive feedback works in a similar manner to contact mode, by keeping amplitude constant while scanning.

Pros of intermittent contact mode:

- The tip does not scratch the surface, thereby avoiding artifacts. This is extremely important for soft samples.
- The tip typically does not remove parts of the sample.
- The Tapping regime allows the collection of various kinds of information related to the properties of the surface material (phase contrast).

Cons of intermittent contact mode:

- Successful use of this mode requires extensive operational skill and additional hardware.
- The load force typically cannot be precisely controlled, in particular in liquid environments.
- To attain good imaging quality, expensive cantilevers must be used.
- The mode does not allow for fast scanning (typically 0.5–2 seconds per scan line).

Because of its nondestructive scanning, tapping mode is a natural choice for the imaging of soft biological surfaces. It normally requires rather stiff cantilevers (spring constants in the range of  $1 \text{ Nm}^{-1}$  and above).

### 1.2.3. Force Mode

Force mode not an imaging mode; it is used to measure forces acting between AFM tip and the surface of interest at a specific point. In contrast to the previous modes, the cantilever does not move in lateral direction. The scanner goes up and down, elevating and approaching the cantilever to the surface. As a result, the image shown in Figure 2 is a typical example of what is recorded. The force  $F$  of the bending of the cantilever (vertical axis) is plotted against the vertical position  $z$  of the sample. When the tip is far away from the surface, there is no deflection, and consequently, the force is equal to zero (there is an assumption of no long-range forces). When the  $z$  position of the sample increases (the sample is moved up by the scanner, Fig. 1), the tip-sample distance decreases. At some point, the tip touches the sample (position of contact). After that, the tip and sample move up together. This part of the force curve is called the *region of constant compliance*. At some point, which can be controlled by AFM operator, the sample stops and retracts down. The force curve before this point is called the *tip-approaching curve*, or simply the *approaching curve*. The force curve recorded when the sample is retracted down is known as the *tip-retracting curve*, or simply the *retracting curve*. During retraction the surface may display non-trivial

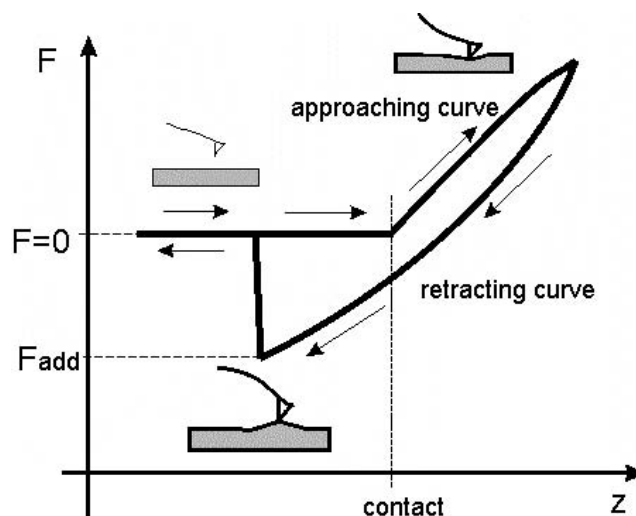


**Figure 2.** A typical force–distance curve recorded by AFM in force mode. Both the approaching and retracting curves are shown.

viscous and elastic properties. This typically results in hysteresis between the approaching and retracting curves, as shown in Figure 2.

One more interesting feature of the retracting curve is the non-zero force required to disconnect the tip from the surface. This is the so-called *adhesion force*. It appears due to weak short-range forces (such as van der Waals forces) acting between the tip and surface while in contact.

Pros of force mode:

- Provides information about surface viscoelastic and elastic properties.
- Also able to detect long-range forces.
- Information about tip-surface adhesion force is recorded.

Cons of force mode:

- No topographical information is recorded.
- Requires a very clean, homogeneous surface. Samples placed in biological buffers cannot be this clean. Moreover, biological surfaces are typically intrinsically heterogeneous. To get reliable force information, one needs to collect and analyze a large amount of force curves.

It is important to note about this mode that the absolute value of the force can be calculated with high precision. However, only the relative position of the sample can be well defined on the soft samples. This appears because of ambiguity in the definition of the tip-surface contact.

To measure surface mechanics, one needs to choose a cantilever with the right spring constant, which should be of the same order of magnitude as the surface stiffness (*surface spring constant*).

### 1.2.4. Force–Volume Mode

This mode was introduced [51] to solve the problems of force mode, described just above. As was noted in the previous section it is useful to simultaneously record the topology of the surface and force curves. Moreover, it is important to do multiple measurements to get reliable statistics. The

question is, how many measurements have to be done to get a definite answer for cell rigidity? While there is no any predefined answer to this question, one can estimate the amount of measurements to be 100 per cell. This has to be repeated for from 10 to 50 cells from a single cell source, and ideally to do this for cells from three different sources. This results in 1,000 to 15,000 measurements. Obviously, this is impractical to do without automation.

Moreover, it is impossible to determine the Young's modulus of the sample (a measure of its stiffness, or, alternatively, its elasticity) without knowing the geometry of the surface near its contact with AFM tip. If the surface were ideally flat, then it would be irrelevant at what point to measure forces. In the case of biological cells, knowledge of geometry is important because cells are not necessarily flat. Therefore, one will need some kind of automatic collection of data on forces and the geometry of the surface at the same time. This can be done in the so-called *force-volume mode*.

"Classical" force-volume mode is implemented in many AFMs. There are different options regulating how this mode works. Below we describe only one of the most relevant set of options, in a typical set-up. While working in force-volume mode, AFM cantilever starts traveling down from a definite distance away from the surface (known as the so-called *ramp size*), moves straight down (with no lateral motion) until the tip touches the surface, and the cantilever deflection reaches some definite level (called the *trigger level*). After that the motion of the cantilever is reversed. The AFM scanner pulls the cantilever straight back to a distance equal to the ramp size. Both the approaching and retracting curves are recorded during such cycle. Then, still away from the surface at the ramp size distance, the tip advances in the lateral direction to a certain distance, and force curves are again recorded, as described above. This operation continues until the tip completes rastering a square area of the sample. Topographical information in such "scanning" is also recorded because the trigger level (i.e., the required cantilever deflection) is reached faster on the hills and slower in the trenches.

Thus, both topography and force curves are recorded at a number of points, or pixels, over the sample surface. Typically this is recorded as a square matrix of, for example,  $16 \times 16$ ,  $32 \times 32$ , or  $64 \times 64$  pixels. The amount of information recorded in a single force-volume file is generally limited. It means that each force curve can be recorded as a limited number of points. In the Veeco Instruments Nanoscope software, up to version 5.12, the number of points is limited to 512, 256, and 64 per force curve for  $16 \times 16$ ,  $32 \times 32$ , and  $64 \times 64$  number of pixels, respectively. A newer version 6 software allows working with up to  $128 \times 128$  pixels for force curves recorded with 128 points each. There are the following advantages and disadvantages of this mode.

Pros of force-volume mode:

- It has all pros of the force mode.
- Topographical information is recorded simultaneously with force curves.
- It allows the collection of a large amount of data to ensure robust statistics. It does not require a very clean homogeneous surface. Therefore this mode is very suitable for biological surfaces that are typically intrinsically heterogeneous.

Cons of force-volume mode:

- It requires a large amount of time to collect the data. This is due to the fact that each force curve is collected for some amount of time. Faster collection is not possible due to viscoelastic effects.
- Only a limited number of data points per force curve can be collected.

Definitely the topography recorded in the force-volume mode carries the signature of surface deformation. This is however also true for any AFM scan of surface. The deformation has to be taken into account while processing the data. Fortunately cells have enough flat areas. Therefore knowledge of this topography can be used simply as a filtering rule, which allows one to choose only those force curves that are recorded on relatively flat areas. For the sake of safety of the cantilever, it is recommended to use so-called *relative trigger mode*. In such mode the cantilever stops approaching the surface when it deflects up to the trigger level *relative* to its initial position at the ramp distance from the surface.

It should be noted that similar-looking mode, called *pulse mode*, was introduced later. However, this mode is not suitable for force measurements. The AFM cantilever oscillates too fast, mixing the force signal with liquid damping. In addition, the cantilever moves up and down independently of the lateral motion of the sample. This leads to possible contribution of the lateral forces to the total force signal near and after the contact.

### 1.3. Advantages of AFM in Biology

The AFM technique has a number of features of that makes it extremely valuable in biology. The main beneficial feature is its ability to study biological objects directly in their natural conditions—in particular, in buffer solutions, *in situ*, and *in vitro*, if not *in vivo*. There is virtually no sample preparation, apart from one requirement, the object of study should be attached to some surface. There are virtually no limitations on the temperature of the solution/sample, chemical composition, and the type of the medium (can be either nonaqueous or aqueous liquid). The only limitation on the medium exists for the most popular optical systems of detection: the medium should be transparent for the laser light used for the detection.

Lateral resolution of AFM on rigid surfaces can approach the atomic scale [52–56]. While scanning soft, in particular biological, surfaces, AFM can achieve resolution of about 1 nm [25, 57–62]. The vertical resolution is mostly determined by AFM detection sensitivity and by environmental noise. Typically it can be as high as 0.01 nm.

To summarize, AFM has the following advantages to study biological objects:

- AFM can get information about surfaces *in situ* and *in vitro*, if not *in vivo*, in air, in water, buffers, and other ambient media.
- It can scan surfaces with up to nanometer (molecular) resolution, and up to 0.01 nm vertical resolution.
- It provides true 3D surface topographical information.
- It can scan with different forces, started from virtually zero to large destructive forces (making "surgery;" see, e.g., Firtel et al. [174]).

- Detection up to single-molecule forces is feasible.
- It allows measuring various biophysical properties of materials, such as elasticity, adhesion, hardness, friction, etc.
- Minimum preparation of the samples is required. For example while scanning cells in a Petri dish, one needs just a change the culture medium to any physiological buffer.

AFM is broadly used to study cell morphology [58, 63–70, 173]. Mechanical properties of cells have been studied by a number of investigators [39, 40, 51, 71–83] (the foregoing offer a number of references therein of other such investigations). In the next section we will describe applications of AFM in studying cancer cells.

## 2. AFM IN STUDY OF CANCER CELLS: GENERAL OVERVIEW

Oncogenically transformed cells differ from normal cells in terms of cell growth, morphology, cell–cell interaction, organization of cytoskeleton, and interactions with the extracellular matrix [84–99].

Atomic force microscopy is capable of detecting most of these changes. It is interesting that in the majority of these applications AFM has not been used as just straight microscopy. However, there are several studies in which AFM is used as a complementary microscopy technique; see, e.g., Barrera et al. [4] and Kirby et al. [173]. In another study, AFM was used as a highly sensitive microscope for early detection of cytotoxic events [7]. In others [9, 16], AFM was used as a high-resolution detector of erosion of collagen substrate surface caused by cancer cells. Apart from these applications, confocal microscopy (fluorescent optical, in particular) is still superior to AFM for overall imaging of cells. Using these optical techniques, one can identify many cancer cells by means of immunofluorescent tags, or just by looking for generally larger than normal nuclei (in proportion to cell size). Optical imaging is quick and provides robust statistics. The real advantage of AFM comes from its following features: ability to detect surface interaction, extremely high sensitivity to any vertical displacements, and capability to measure cell stiffness and mechanics. We will overview three main directions in AFM study of cancer cells below: atomic force spectroscopy, sonocytology, and cellular mechanics. We will briefly summarize advantages and potential problems of using AFM for those particular applications.

### 2.1. AFM Detection of Surface Interactions (Atomic Force Spectroscopy)

It has been shown that AFM is capable of detecting interactions between single molecules attached to AFM tip and surfaces of interest. This mode of operation is typically called atomic force spectroscopy [22, 100–104]. Subsequently, AFM can be used to identify ligand-receptor interactions on the cell surface, which can be specific for different cancers [8, 13–15, 30, 33–35, 105]. While fluorescent markers are broadly used in biology to identify specific ligand-receptor affinity, AFM has an advantage in that it

measures the forces involved directly. It allows the recording of complete force distance curves as well as information about the forces needed to disrupt molecules stuck together (adhesion forces).

While it is unlikely that AFM can compete with immunofluorescent detection, knowledge of forces should be of interest in understanding the nature of ligand-receptor interactions. The AFM can also attain considerably higher resolution, especially along the vertical axis, when comparing with confocal microscopy. Describing precise methods of atomic force spectroscopy on cancer cells is beyond the scope of this review. We can refer the readers to a host of original literature [8, 13–15, 22, 30, 33–35, 100–105].

We can summarize this application as follows:

Pros of atomic force spectroscopy:

- Can obtain high-resolution force information about ligand and receptor interaction.
- Complete force distance curves and statistics of molecular disruption can be measured.

Cons of atomic force spectroscopy:

- Time- and labor-consuming AFM tip preparation.
- Smaller cell statistics in comparison with immunofluorescent methods.

### 2.2. Cellular Sound (Sonocytology)

An interesting application has been developed recently. Using the high sensitivity of AFM to vertical displacement, Dr. James K. Gimzewski's group found that the cell membrane oscillates in the kilohertz range. These vibrations can easily be detected with a standard AFM setup. The signal can be processed as a regular sound signal, and consequently, amplified up to the level of audible sound [37]. This method is called "sonocytology." It was discovered that cancerous cells emit a slightly different sound than healthy cells do. It is potentially a very interesting application, which may someday results in early cancer detection. It should, however, be noted that this method has been developed *in vitro*. Expanding such measurements for applications *in vivo* is not a trivial task.

It is also worth noting that the idea to use sound (even "music") of oscillating cells to distinguish between normal and cancer cells is not new. It was suggested by Giaever a few years ago. The idea was based on cell oscillations detected as differences in measured electrical impedance [106]. Those data were also collected *in vitro* (though the data recorded were in a different frequency range, and consequently, were processed differently to get an audible sound). To the best of the author's knowledge, no further development study has been reported after that time.

We can summarize this application as follows:

Pros of sonocytology:

- It is potentially an easy and elegant method of cancer detection and prophylaxis.

Cons of sonocytology:

- It is hard to distinguish the sound difference between normal and cancer cells unambiguously.
- In the long run, it will be necessary to extend the method to *in vivo* applications, which is not a trivial task.

### 2.3. Cell Mechanics

In studying cell mechanics, AFM has a unique advantage. Lateral position of AFM tip, as well as the load force can be controlled with extremely high precision [1, 5, 42, 107]. The AFM records strain-stress characteristics (force deformation curves) on the area which can be as small as a few nanometers in diameter (tip contact). This can be done on individual cells or cell layers in a Petri dish (*in vitro*), or even on pieces of tissue (*ex vivo*). It should be noted that there are a few other probe methods used to study cell mechanics. The most popular are optical tweezers [47, 108, 109], magnetic beads [110–120], and micropipette [121–128]. However, those methods cannot compete with the precision that can be attained with AFM method.

Why are mechanics of cells of interest? Correlation between elasticity of tissue and different diseases has been known for a long time. It has been implicated in the pathogenesis of many progressive diseases including vascular diseases, kidney disease, cataracts, Alzheimer Disease [129, 130], complications of diabetes, cardiomyopathies [131], and so on. However, it is believed that in many cases the loss of tissue elasticity comes from rigidification of the extra cellular matrix [132], not the cells themselves. But recently it has been shown that the cells can also change the rigidity quite considerably [133]. By now there are several studies reported on measurement of rigidity of cancer cells [19, 20, 27, 29, 134], which show quite a difference from normal cells. While the differences are clearly seen, the reason for that is far from being understood. We will describe those results in the next section in more detail.

It was recently found that the mobility and the spreading of cancer cells may indeed be regulated by the application of external forces [23, 36]. This may result in some major breakthrough in cancer screening and diagnosis. While in those works researchers were focused on the tumor tissue in general, and attributed the stiffness change to entirely extracellular matrix, it will be definitely of interest to look at individual cell level.

We can overview this AFM application as follows:

Pros:

- It provides unique ability to record strain-stress characteristics on individual cells the with nanometer resolution.
- Simultaneous collection of topological and mechanical data is possible.
- It has the ability to collect both static and dynamic (visco) elastic data.
- It can work with samples *in vitro* as well as *ex vivo*.

Cons:

- One needs to control a large number of possible parameters related to AFM method and preparation of cell culture (see the detailed description later).
- It is necessary to collect large amount of data to attain robust statistics.

## 3. AFM IN STUDY MECHANICS OF CANCER CELLS: DETAILS

Cell mechanics can be studied with AFM in two regimes: static and dynamical measurements. The static measurement

is done when the probe deforms the cell surface rather slowly. In dynamical measurements, the probe oscillates with high frequency. In the case of elastic materials (cells are typically the one), static measurements can be understood in terms of Young's modulus of rigidity. The dynamical measurements are characterized by two rigidity moduli, storage and loss (see, e.g., Mahaffy et al. and Bippes et al. [31, 135]). Because dynamical measurements are frequency dependent, both moduli can depend on the frequency. Obviously, dynamical measurements provide more information than static measurements. However, for now almost all studies of cancer cells are static. This can be explained by difficulties in both experimental setup/control and theory to process the data. Moreover, the reason for observed differences between normal and cancer cells even in the static case are still not entirely clear. In this work we will focus on static measurements of rigidity only.

To do the measurements, one needs to move the probe with some final speed even in the case of the static regime. This is why this type of measurement would be better called *quasi-static*. From the practical point of view, however, it is rather simple to find the appropriate speed of oscillation of the AFM probe. Both the approaching and retracting curves should be about the same after the contact (the region of constant compliance; see the description of force mode, Section 1.2.3). If they are not the same, as in the case of the example shown in Figure 2, then we are dealing with viscoelastic response. The speed of oscillation should be decreased until those parts of the curves merge together. In some cases, however, it is impractical to do because it would take too much time to collect enough data necessary to get robust statistical information. In any case, it is useful to keep and report information about the speed of the probe oscillation used in the measurements.

One important remark should be made here. The cell is not a homogenous medium. However, as has been shown in the literature [136–139], the approximation of a homogenous medium works surprisingly well to describe the mechanical properties of cells. Therefore, Young's modulus of rigidity can be used to describe such medium.

### 3.1. Rigidity of Cells: Where we are in Numbers

It is useful to understand the range of cell rigidities that researchers can deal with. Obviously cells are softer than many materials one is used to dealing with every day. It is trivial to see by poking cells with a sharp pipette under an optical microscope. Quantitative measurements [1, 11, 40, 41] show the position of cells on the Young's modulus chart, Figure 3. One can see that the cells are indeed softer than other materials typically in use in biology. There is considerable variation of rigidity within cells of different type. Epithelial cells seem to be the softest ones. Edge of young epithelial cell can have a Young's modulus of  $\sim 0.2$  kPa [133]. Platelets are the toughest with Young's modulus as high as hundreds of kilopascals.

When measuring cell mechanics, it is of paramount importance to do multiple measurements to gain enough statistical knowledge. It is not a trivial statement for many physicists and chemists. Intrinsic variability of biological

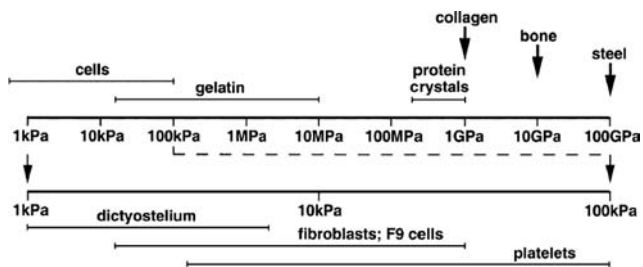


**Figure 3.** The Young’s moduli of different materials. The diagram shows a spectrum from very hard to very soft: steel > bone > collagen > protein crystal > gelatin, rubber > cells. Note a considerable variation of rigidity even within cells. Reprinted with permission from [1], J. L. Alonso and W. H. Goldmann, *Life Sciences* 72, 2553 (2003). © 2003.

forms is considerably higher than typically known in either physics or chemistry. Furthermore even within one cell there are different areas of rigidity, which can be different by orders of magnitude [25, 133, 140]. For example, as was shown in Berdyeva et al. [133], the difference in rigidity at the cytoplasmic area and cell edge can have more than two orders of magnitude. The next factor of uncertainty can be the cell age and its mitosis stage. It was demonstrated [141] on normal rat kidney (NRK) fibroblasts (ATCC) cells that the Young’s modulus of the middle (between nuclei) of dividing cell changes from ~1 kPa (during interphase) to ~10 kPa (during cytokinesis). Results of Berdyeva et al. [133] show that a similar change in rigidity (about 10 times) can be observed on epithelial cells while aging *in vitro*. Finally, the Young’s modulus can depend on the depth of probe penetration. Without the special analysis and modeling of cells as a multilayered shape, one obviously can speak about the effective Young’s modulus of the cell only. All of these problems demonstrate that one has to be very careful in choosing the appropriate cell model to study cell rigidity. These and other issues will be discussed later.

### 3.2. How to Measure Rigidity of Cells with AFM: Experimental Steps

Cell rigidity can be measured using force mode, which was described in the Introduction. As a result of measurements in the force mode, one gets a force curve (force vs. *z*-position of the sample). An example of two such measurements done on two surfaces of different rigidities is shown in Figure 4 (only approaching curves are shown). After contact, the AFM tip touches the surface and the cantilever deflects up. The corresponding force, plotted in Figure 4, is equal to the cantilever deflection multiplied by the spring constant of the cantilever. If you have two different surfaces, one softer and one harder, there is larger deflection of the cantilever on harder surface. This is because the harder surface pushes the cantilever up stronger, while the softer surface lets the cantilever penetrate deep inside. Thus, measuring the slope of the force curve after the contact (region of constant compliance), one can get information about surface rigidity.

Using these force curves (sometime called *indentation curves*), one can easily calculate the *stiffness*, which is defined as a derivative of force *F* with respect to penetration *p* (indentation),  $dF/dp$ . To calculate penetration, one can use

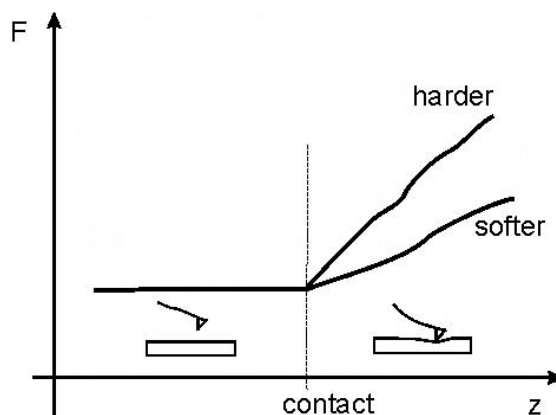


**Figure 4.** Force–distance curves for two materials of different rigidity. Only approaching curves are shown.

a simple formula  $p = z - d$ , which can be obtained from straightforward geometrical considerations. Here *d* is deflection of the cantilever (positive when it deflects up), and *z* is the vertical position of the sample (and is equal to zero at the moment of the tip-sample contact). While stiffness is a rather well-defined characteristic of surfaces, it is not a clear characteristic of materials. Stiffness depends not only on Young’s modulus of rigidity (which is a material characteristic), but also on the geometry of the tip-surface contact. Therefore, to be able to compare different materials, one needs to deal with Young’s modulus of rigidity, which is independent of the tip geometry. How to calculate Young’s modulus will be described in the next sections. Below we will describe the major experimental steps needed to measure mechanics of both normal and cancer cells. Because there are too many experimental approaches in studying cell mechanics, description of such steps is very important. Eventually it may be promoted as a sort of protocol, the researchers able to compare the mechanics of a large variety of different cells.

#### 3.2.1. Cell Culture Preparation

Before imaging, cells should be attached to some rigid substrate, usually either a slide or the bottom of a Petri dish. It is recommended to use specially coated dishes or slides to facilitate adhesion. Such Petri dishes or slides are available commercially, or can be prepared by coating with various molecules that have suitable amino groups, see, e.g., Sagvolden et al. [43]. After that the slide/dish has to be mounted on the AFM stage, for example with double-stick tape. Size of the Petri dishes is also important to have convenient measurements. Working with larger Petri dishes requires the removal of a part the dish side, which is extremely inconvenient.

Right before placing the cells in the AFM for analysis, the culture medium should be replaced by a balanced buffer which does not contain proteins. Phosphate-buffered saline (PBS) or Hank’s buffered saline solution (HBSS) are good choices. Working at room temperature, the cells are typically viable in these buffers for a few hours. For example, we found that human epithelial cells can survive at least

3–4 hours in HBSS and at least 2–3 hours in PBS solution. Obviously this time will decrease if working at elevated temperatures.

### 3.2.2. AFM Probe Preparation

To measure the rigidity of such materials, virtually any regular AFM cantilevers can be used. Spring constants can be in the broad range of  $0.001\text{--}100\text{ N m}^{-1}$ . The optimum spring constant should be approximately equal to the effective spring constant, or stiffness, of the surface. Because cells are soft, a possible AFM tip penetration can be quite large. The part of the tip which is in contact with the cell will also be large. Consequently, that part of the tip shape has to be well-defined. A standard AFM tip is rather sharp. Tip penetration is typically much larger than the radius of the tip apex. Therefore one needs to know the tip geometry in larger scale. A regular AFM tip has a cone geometry on the larger scale. Such tips have been widely used [19, 20, 26–29, 40, 134, 142] to study cells. The major problem with such tips is that they induce too large a stress in the vicinity of the tip apex [143, 144]. Such a large stress can lead to nonlinearity in the material response. The second major issue with sharp AFM tips is the relatively small area of contact. Cells can have rather inhomogeneous surfaces. Structural cytoskeleton fibers can sit directly underneath the cell surface. When the area of contact is small, the tip can be either right above the fibers or between the fibers. As a result, measured rigidities can vary broadly. To get robust statistics, one needs to do too many force measurements. At the same time, one has limited time in the experiment to maintain viability of cells.

The solution to the above problems is in using well-defined dull tips. Such tips can be made by gluing a colloidal spherical particle to the AFM cantilever [133, 144–147]. Figure 5 shows an example of a V-shaped standard AFM cantilever with a  $5\text{-}\mu\text{m}$ -diameter silica ball glued with epoxy resin. One can clearly see a big difference in the area of contacts of a regular pyramidal tip and the silica ball. In general it is easier to use special tipless cantilevers for the attachment of such large colloidal probes.

The larger area of probe-cell contact results in averaging local variation in rigidity compared to that measured with a regular sharp probe. On some type of epithelial skin cells, we measured the standard deviation in the distribution of Young's modulus up to 200–300% when measuring with regular integrated pyramidal silicon nitride tips (DNP-S by Veeco/DI Inc.). That spread was reduced almost by an order of magnitude when using silica ball tips. Although for some other types of cells this difference is not that pronounced. Overall reduction of the spread is greatly helpful for attaining robust statistics of measurements.

There is a couple of other advantages of using colloidal probe particles. Due to the low rigidity at thin edge of some cells, it would be very hard, if not impossible, to make measurements with a sharp AFM tip. The sharp tip simply penetrates the thin areas of the cell and shows even higher rigidity due to touching the rigid substrate. Using colloidal probe particles such thin areas can easily be measured.

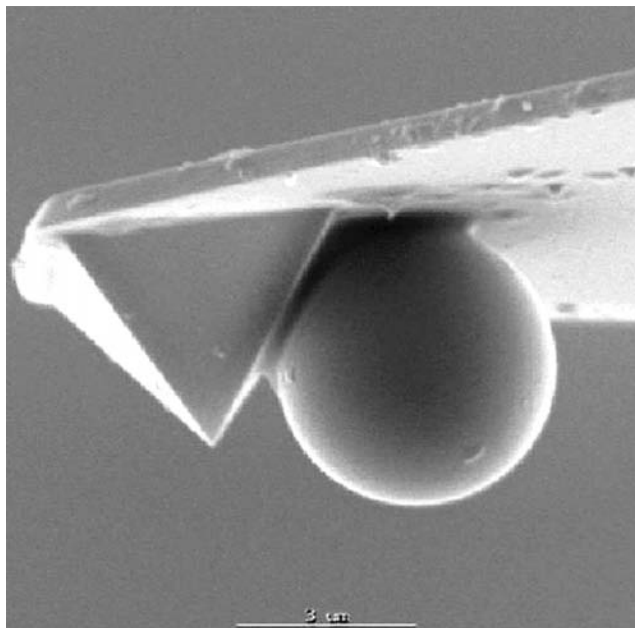


**Figure 5.** An example of a V-shaped standard AFM cantilever (apex diameter, 50 nm) with a  $5\text{-}\mu\text{m}$ -diameter silica ball glued with epoxy resin. Reprinted with permission from [133], T. K. Berdyeva et al., *Phys. Med. Biol.* 50, 81 (2005). © 2005.

### 3.2.3. Tip Geometry and the Cantilever Spring Constant

To extract the information about the Young's modulus of rigidity from measured data, one needs to know the cantilever spring constant and exact tip geometry. The radius of the probe and its cleanliness can be tested by scanning the reverse grid (TGT01, Micromash, Inc., Estonia), and sometimes with SEM. TGT01 grid is a set of very sharp silicon tips which have radii of the apex less than 5–10 nm, Figure 6, left. Scanning over such tips with the large colloidal probe results in a kind of “inversed” image of the probe. Effectively, the sharp AFM imaging tip is now attached to the surface, and the colloidal probe plays the role of a sample. The image of colloidal probe is produced by each silicon tips. An example of a  $5\text{ }\mu\text{m}$  silica ball probe scanned over the sharp silicon needles, the reverse grid is shown in Figure 6, right image. Processing this data with any software that allows non-linear

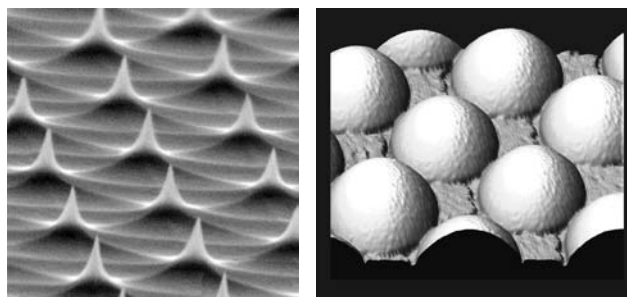


**Figure 6.** An SEM image of TGT01 grid (left image; Reprinted with permission from MicroMash, Inc., Estonia). Reverse grid image of a  $5\text{-}\mu\text{m}$  silica ball attached to AFM cantilever.

curve fitting, one can find the radius of AFM probe attached to the cantilever.

The cantilever spring constant can be found using different procedures described in a host of literature [147–153]. Using V-shaped cantilevers from Veeco/DI, one can utilize a built-in option of the Nanoscope software to find the spring constant of the cantilever. The newer versions of the Nanoscopes software contain implementation of another method which is based on thermal fluctuation analysis. That method is more cantilever-shape independent, but can be applied only to sufficiently soft cantilevers.

### 3.2.4. Cantilever Sensitivity Calibration

This is the first necessary step before making actual measurements. Deflection of the cantilever is detected by either a photodiode or a piezosensor (piezolever). Both detectors give readings in electrical units, i.e., Volts. However, for the force measurements one needs to get the cantilever deflection in the units of length, i.e., meters (or nanometers). The coefficient that converts Volts into meters has to be measured each time after aligning the laser on the cantilever (or changing the piezolever). Finding such a coefficient is called sensitivity calibration of the cantilever. Specific technical realization of such calibration can depend on AFM manufactures. However in all cases, this can technically be done by recording a force curve on a sample that can be treated as absolutely rigid material. In that case, both the tip and simple surface move together after the contact. Because the shift of the sample (in the units of length, nm) is known, one has to equalize it to the change in the voltage of photodiode (in the units of voltage, Volts).

It is best to perform the calibration prior to performing an experiment because the cantilever may become damaged during the experiment. If this occurs, then one can no longer do the calibration and the recorded force data can be lost. Secondly, the obtained spring constant can reveal possibly damaged cantilever. In the later case, one would observe noticeably less spring constant than its nominal value typically given by the manufacturer.

It is useful to note that the photodiodes used in AFMs are fairly linear with respect to the position of the laser spot. Therefore, realigning the position on the photodiode (detector) with respect to the laser spot position does not require recalibration.

### 3.2.5. Using Force–Volume Mode

Having calibrated the cantilever, one can start collecting force data. The tip can be located above the cell with the help of any optical system. For example, one AFM has a built-in optical video microscope, which allows observation of areas from  $150\ \mu\text{m} \times 110\ \mu\text{m}$  to  $675\ \mu\text{m} \times 510\ \mu\text{m}$ , with  $1.5\ \mu\text{m}$  resolution. Simultaneous position of the tip can be done with lateral accuracy of  $\sim 10\ \mu\text{m}$ . Before going to the force–volume mode, a single good force curve should first be obtained. To get such a curve, one should use the force mode. The goal of this step is to optimize the variety of parameters of the force mode such as the ramp size and the trigger level (see above). After optimizing the parameters and recording a good force curve, one should proceed

to the force–volume mode to collect large amount of the force data.

The important parameters in the force–volume mode are the number of pixels on the cell surface in which the force information will be recorded, and the speed of oscillation of the AFM tip. Typically, the choice of the oscillation speed is a compromise between the duration of the data collection and working in the regime where the viscoelastic effects are not very pronounced. The number of pixels should be sufficient to distinguish the variability of stiffness over the cell surface, as well as topography of the surface itself.

One note should be mentioned about a possible range of the ramp size. It is restricted by the maximum range of the scanner in the vertical direction. If one uses the relative trigger mode (recommended option for the safety of the cantilever), the maximum size is only the half of the maximum scanner range. This creates a problem for a majority of AFM scanners because the cells have heights which are normally quite large. To avoid this problem, the area of the whole cell can be split into a series of small areas; each of those has suitable height variation. The measurements should be done on each of these small areas. Alternatively, a new scanner with a larger vertical range is needed. Fortunately, such scanners are commercially available. To be sure that the scanner is free of possible nonlinearities at such a large scale, the closed-loop type of scanner is recommended.

### 3.2.6. Control Experiments

The purpose of such experiments is to exclude any changes in rigidity which could be artifacts of imaging or culture preparation. There can be a number of such experiments. Section 3.5.3 below describes different sources of uncertainty and possible alteration of cell rigidity due to either culture preparation or AFM technique itself. The control experiments that have to be done depend on the cell type. Below we describe an example of such a control experiment performed in the case of human skin epithelial cells.

Poking a cell with the AFM tip during measurements can potentially cause internal changes in the cell. There is some evidence [142] that the tip can cause alteration of the cytoskeleton. Different types of cells can have different responses to the action of the AFM probe. Therefore, it is logical to conduct a controlled experiment, continuously measuring mechanical properties of the cell during scanning in the force–volume mode. For example, as was shown elsewhere [133], the AFM probe continuously measured (in force–volume mode) a cell along the same line at 32 points for about two hours. No significant change in rigidity was detected. It should be noted that small alterations in Young's modulus may be a result of gentle force–volume scanning. This is not necessarily the case for the contact or Tapping imaging modes of scanning, where both relatively large vertical and lateral drag forces are applied to the cell.

## 3.3. How to Measure Cell Rigidity with AFM: Young's Modulus Calculations

After the collection of data, it should be processed. In this section we consider different models to extract Young's

modulus of rigidity from the force curves measured as described above. To find Young's modulus, one needs to know the tip geometry and structure of the sample. The tip geometry can be found as described above. However, the structure of the sample is too complicated to be treated without any assumptions. Here we will assume that the cell is a homogeneous, isotropic medium. Obviously this is an approximation. There is a plethora of literature showing that such an approximation is plausible [19, 20, 26–29, 40, 134, 136–139]. We will demonstrate this in more detail later in this section.

Configuration of a spherical probe over a flat homogeneous surface is described by the Hertz–Sneddon model [107, 154, 155]. This model was developed for either a spherical probe of radius  $R$  or a parabolic tip over a plane surface. In the case of a parabolic tip described by equation  $Z = b \cdot X^2$ , the effective radius  $R$  can be found as  $1/2b$ . In this model, the Young's modulus  $E$  is given by

$$E = \frac{3}{4} \frac{1 - \nu^2}{\sqrt{R}} \frac{dF}{d(p^{3/2})} \quad (1)$$

where  $F$  is the load force,  $R$  is the radius of the ball,  $p$  is the probe penetration into the cell. The Poisson ratio  $\nu$  of the cells is unknown. For the majority of biological materials,  $\nu = 0.5$ . Nonetheless, we will treat the Poisson ratio to be unknown. To remove this uncertainty, we will speak about an “apparent” Young's modulus, to be defined as follows

$$E_{\text{app}} = \frac{E}{1 - \nu^2} \quad (2)$$

In the derivation of Eq. (1) it was assumed that the rigidity of the probe is much higher than the rigidity of the sample. This is generally true for the majority of AFM probes. The Hertz–Sneddon model has also two additional assumptions. The first one is that the probe penetration into the sample should be much smaller than the radius of the probe. This can easily be controlled. The second assumption is about the lack of adhesion between the probe and sample surface. Looking at the force curves, one can easily identify the adhesion ( $F_{\text{add}}$  in Fig. 2). If the adhesion is high, one has to use another model, the so-called JKR (Johnson–Kandall–Roberts) model [156–161] to find the Young's modulus. The material of the probe can be chosen, or altered to ensure low adhesion. Typically the adhesion between an AFM probe (for example, a clean silica sphere) and a cell is low. Therefore, we will not describe the JKR model here, referring the reader to the original literature [156–161].

The majority of standard AFM cantilevers have a conical shape. It is useful to present a result of application of the Hertz–Sneddon model to a conical probe. For a conical tip with a semivertical (opening) angle  $\alpha$ , the apparent Young's modulus can be given by the following formula

$$E_{\text{app}} = \frac{1}{2} \pi \tan \alpha \frac{dF}{d(p^2)} \quad (3)$$

Let us show an example of the application of the Hertz–Sneddon model to an epithelial cell. It is well known that the cell is a very complicated object from a structural point of view. Nevertheless as we have already mentioned,

it is surprisingly well described by the approximation of a homogeneous medium. From the general point of view such an assumption is not that unexpected if we deal with small deformations. However, for larger deformations this assumption is obviously broken. According to Eq. (1), a plot of the load force versus the probe penetration to the  $3/2$ th power must be a straight line. Figure 7 demonstrates the results of processing about 30 force curves averaged over an edge of epithelial cell [133]. (The approach force curves were used here. A  $5\text{-}\mu\text{m}$  silica ball was used as a colloidal probe.) One can see in Figure 7 that the Hertz–Sneddon model is a good approximation until  $p^{3/2} = 4000 \text{ nm}^{3/2}$ , which corresponds to a penetration of  $\sim 250 \text{ nm}$ . It is interesting to note that for sufficiently large penetrations, the Hertz–Sneddon model starts working again. One can see in Figure 7 that the force- $p^{3/2}$  curve can again be approximated by a straight line after a penetration of approximately  $500 \text{ nm}$ . This is yet to be understood.

### 3.4. Mechanics of Cancer Cells: Results

The results we discuss below are summarized in Table 1 in historical order. One of the first measurements on a cancer cell line was done on human lung carcinoma cells [134]. It showed quite a variation in the measured Young's modulus,  $13\text{--}150 \text{ kPa}$ , and was essentially a demonstration of the method. Such variability in the modulus is presumably a result of the few statistics collected during these measurements. This is explained by the fact that the authors did not use automated tools such as the force–volume mode, and had to collect individual force curves. A sharp AFM tip was used in this study.

An interesting analysis of the rigidity of cancer cells (wild, and vinculin-deficient, (5.51) mouse F9 embryonic carcinoma cells) has been done [19, 20]. The authors compared wild-type mouse F9 embryonic cells, which can

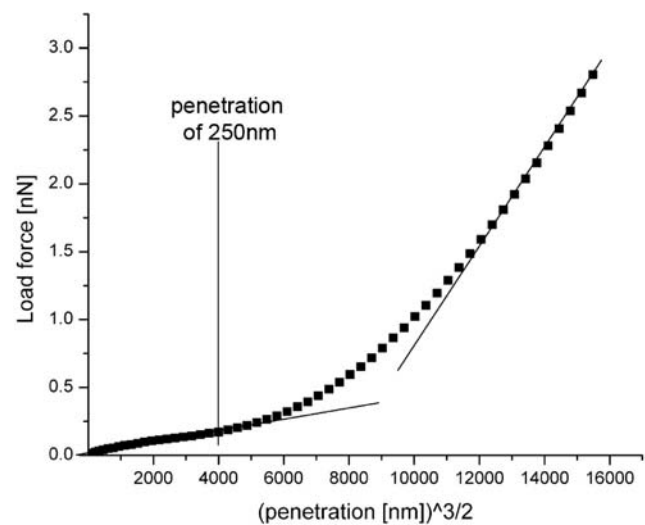


**Figure 7.** Plot of probe penetration to the 1.5 power versus load force. According to Eq. (1), a straight line demonstrates constancy of the Young's modulus, and therefore represents validity of the model. Reprinted with permission from [133], T. K. Berdyeva et al., *Phys. Med. Biol.* 50, 81 (2005). © 2005.

**Table 1.** Summary table of measured apparent (i.e., where Poisson's ratio = 0) Young's moduli of cancer cells (with some normal strain). Asterisk (\*) denotes data taken from Figure 7 of Park et al., with permission of the publisher [162].

Cell: tissue type	E [kPa]	Note	Ref.
Human lung carcinoma cell	13–150	Cells were collected from a 62-year-old individual. Single force–distance curves were used in analysis. Sharp AFM tip was used.	[134]
Mouse F9 embryonic carcinoma	$3.8 \pm 1.1$	Correlation between rigidity and vinculin deficiency was studied further by vinculin transfection. This confirmed gradual decrease of rigidity with the decrease of vinculin expression. Force–volume mode was used. Sharp AFM tip was used.	[19, 20]
Vinculin-deficient mouse F9 embryonic carcinoma (5.51)	$2.5 \pm 1.5$		[19, 20]
Hu609 (non-malignant ureter cells)	$12.8 \pm 4.8$ (normal cell)	Ureter and bladder cells are rather similar cell types. About 20 cells of each type were measured. A sort of force–volume mode was used. Sharp AFM tip was used.	[29]
HCV29 (non-malignant bladder urothelium)	$10.0 \pm 4.6$ (normal cell)		
T24 (bladder transitional cell carcinoma)	$1.0 \pm 0.5$		
BC3726 (HCV29 cells transfected with <i>v-ras</i> oncogene)	$1.4 \pm 0.5$		
Hu456 (bladder transitional cell carcinoma)	$0.4 \pm 0.3$	Average over the cell values are shown. Only a few force curves per cell were collected.	[162]
Fibroblast BALB 3T3	$1.3 \pm 1.0^*$ (normal cell)		
Fibroblast: SV-T2	$0.6 \pm 0.5^*$		
Fibroblast: H- <i>ras</i>	$0.5 \pm 0.5^*$		

attach and spread well on extracellular matrix, and vinculin-deficient (5.51) cells, which contain no detectable vinculin protein and spread poorly on substrates. In these measurements the researchers used the force–volume mode to collect enough statistics. It allowed them to calculate the standard deviation of the Young's modulus distribution. Young's modulus of  $3.8 \pm 1.1$  kPa and  $2.5 \pm 1.5$  kPa, was calculated for wild-type and 5.51 cells, respectively. It should be noted that in all these calculations the standard deviation in the distribution comes not from the error of measurements but rather from the intrinsic variability of the modulus distribution over different cells as well as for a single cell surface. Despite the fact that the difference in rigidity was only  $\sim 20$ – $25\%$ , it was further corroborated by studying vinculin-transfected cells. In those cells the amount of stress fiber versus the F-actin mesh was different, and the expected gradual change of rigidity was detected. A sharp AFM tip was used in this study.

It is definitely of great interest to compare the mechanics of normal and malignant cells of the same type. The first comparative study of the mechanics of tumor and normal cells was reported in 1999 [27, 29]. Cells of similar types were studied: Hu609 (non-malignant ureter cells), Hu456 (bladder transitional cell carcinoma cell), HCV29 (non-malignant bladder urothelium cell), BC3726 (HCV29 cells transfected with *v-ras* oncogene), and T24 (bladder transitional cell carcinoma, ATCC HTB4). In that careful study, the researchers collected enough data to derive statistically sound results. The results for Young's modulus of these cells are shown in Table 1. One can see rather substantial differences in rigidity among the various cell types. Cancer cells were reported to be softer than normal cells, by up to one order of magnitude. Moreover, some nonlinearity was detected for normal cells: Young's modulus for the normal strain Hu609 calculated for lower load forces (up to 2 nN) was  $15.2 \pm 4.7$  kPa, versus  $12.9 \pm 4.8$  kPa obtained for large forces (5–10 nN). Young's moduli calculated for cancerous

cell lines were almost independent of the load. Furthermore, for small probe penetration depths (lower than 100 nm), when the influence of the membrane was the highest, the difference between normal and cancerous cells was not visible. The reported method could not distinguish between normal and cancerous cell membrane mechanics, while the difference between normal and cancerous cells was rather clear with the increase of the probe penetration depth.

Recently, local rigidity differences between normal fibroblasts (BALB 3T3) and cancer cells (SV-T2 and H-*ras*-transformed fibroblasts) were investigated [162]. Although that work was focused on the correlation between motility and viscoelasticity of cells, a clear decrease of the Young's moduli of normal and cancer cells was observed. The Young's moduli were measured at about three different points on each fibroblast. Specifically, 38 points from 13 BALB 3T3 fibroblasts, 29 points from 10 SV-T2 fibroblasts, and 18 points from 8 H-*ras*-transformed fibroblasts. Averaged moduli (over three points per cell) are shown in Table 1. There is also a significant difference in the elastic constants of lamellipodia (leading edge of the cell) between normal ( $1.01 \pm 0.40$  kPa) and malignantly transformed fibroblasts whereas there is no significant difference between SV-T2 ( $0.48 \pm 0.51$  kPa) and H-*ras*-transformed fibroblasts ( $0.42 \pm 0.35$  kPa). Normal fibroblasts displayed a much wider distribution of Young's modulus (0.34–4.95 kPa) than the malignantly transformed fibroblasts. There was no occurrence of elastic constants exceeding 3.0 kPa for the malignantly transformed fibroblasts.

It should be noted that a definite difference in Young's modulus at different points on the cell was observed. However, not enough statistics were taken. It is interesting to note that the authors use not only the Hertz model to calculate Young's modulus. More complicated models [31, 163, 164], which take into account a possible influence of the substrate were utilized. The Young's modulus in the thicker cellular regions closer to the cell body (cytoplasmic area),

was successfully derived using the Hertz model. The measure of success here was defined as independence of Young's modulus from the penetration depth. Thinner lamellipodia areas were analyzed with the Tu model or the Chen model [163, 164] due to the substrate effect (which was seen as a strong dependence of the Young's modulus on the penetration depth).

### 3.5. Discussion

#### 3.5.1. General Analysis of the Studied Mechanics

When approaching the cell surface, the AFM probe encounters first the layer of glycocalyx (polysaccharide molecules covering cytoplasmic membrane), then the cell membrane reinforced with a mesh of F-actin, and finally, the deeper cell body. Mechanical differences between normal and cancerous cells in all of these layers can contribute to the measured Young's modulus with the AFM method. Let us analyze the existing data to understand possible influences of these layers.

Note that a sharp AFM tip was used in the first measurements [19, 20, 27, 29, 134]. It is highly unlikely that the layer of glycocalyx could be detected with such a sharp tip. What about the next membrane layer? As has been noted [29], a sharp AFM tip could not distinguish between normal and cancerous cell membrane mechanics, while the difference between normal and cancerous cells was rather clear with the increase of the probe penetration depth. This may mean that there are indeed no detectable differences between membranes in cancer and normal cells, or alternatively, the sharp AFM tip is not capable of detecting such differences. The difference in cortical layer of F-actin is expected for normal and cancer cells [168, 169]. Therefore it is probable that the sharp AFM tip is simply not capable of detecting the difference. This seems to be in agreement with the conclusion of previous works [19, 20]. In those works the authors noted that in wild-type cells, F-actin is organized into bundles (stress fibers) which terminate at focal contacts, whereas vinculin-deficient cells show no actin stress fibers, and instead F-actin is concentrated under the plasma membrane. Based on that, they concluded that rigidity was more influenced by stress fibers (located more deeply in the cell body) rather than F-actin mesh (located immediately under the plasma membrane).

A much larger polystyrene ball of 1–4  $\mu\text{m}$  (1000–4000 nm) in diameter (compared with a diameter of 10–100 nm<sup>1</sup> for the sharp AFM probe) was used as an AFM probe in recently reported measurements [162]. As one can see from Table 1, differences in Young's modulus were clearly detected. However, the differences in the modulus values was nearly the same as the variation within the cancerous cells reported by Lekka et al. [29]. Nevertheless, the analysis by Park et al. [162] was done in a more precise way. To measure an order of magnitude difference in Lekka et al.

the authors did not need too precise a knowledge of the cantilever spring constant and the tip radius. Whereas in Park et al. the spring constant was not assumed but measured to a high precision ( $\sim 5\%$ ), and the tip radius as well (using the methods described here in Section 3.2.3). The high variability of the modulus has still to be understood. A somewhat low number of statistics within each cell (three points per cell) does not allow concluding it is intrinsic variation of Young's modulus.

It is interesting to note one more potential source of variability can be hidden in a rather complicated analysis of the force curve done in Park et al. [162]. The authors found that the force curves measured on thick regions of the cell can be well-described with the Hertz model, i.e., the Young's modulus derived within such a model does vary directly with the probe penetration. However, if the force curves are taken near the cell edge, the Hertz model does not give a constant modulus. This was plausibly interpreted as influence by the cell substrate, and consequently, processed using multi-layered models [163, 164] treating cells as a layer on a substrate. The substrate can be either softer (a gap between a Petri dish and the cell) or harder (the cell on the Petri dish). The major assumption here is that the whole cell was treated as a homogeneous medium with the same Young's modulus. While it is definitely a plausible assumption, in particular, for the thin cell, it "unifies" all cell layers by treating the cell body as homogeneous and isotropic medium. This may bring additional variation in such an overall cell rigidity.

Can we make the conclusion that a large spherical AFM probe is capable of detecting cell membrane/cortical layer? Presumably the answer is yes. For the example of epithelial cells, a very good definition of Young's modulus derived from the Hertz model was observed in Berdyeva et al. [133], in which a 5- $\mu\text{m}$  silica colloidal probe was used. This definition is shown in Figure 7. One can see good definition of the Young's modulus for small penetrations (as well as for large penetrations). As was found in Berdyeva et al., the measured Young's modulus for small penetrations is well correlated with the surface density of fibers in the cortical layer, but less correlated with the total amount of cytoskeletal fibers. This supports our conclusion that the first part of the force curve recorded with AFM colloidal probe is determined by cortical layer of cytoplasmic membrane.

This conclusion can be compared against the recently published study on the rigidity of the dependence between monkey fibroblast cell mechanics and alteration of their cytoskeleton [165]. It is interesting to note that there was a sharp AFM tip used in this study. Unfortunately there was no information given to the radius of the used probe. It was shown [165] that AFM measurements can easily detect the alteration of F-actin and tubulin. Specifically, change in F-actin led to alteration in the initial parts of the force curves, whereas change in tubulin resulted in the alteration of the deeper penetration part of the force curve. Because of the large concentration of F-actin near the cell membrane, cortical layer, this presumably means that even a sharp AFM probe is capable of detecting the contribution from the membrane cortical actin for this type of cell. This statement is however not in agreement with the conclusion of other research [19, 20], in which the conclusion was that the rigidity was more influenced by stress fibers (located more

<sup>1</sup> It should be noted that the sharp AFM tips used in these studies had indeed pyramidal shape, which can be described by a cone model. The effective contact area of such tip is higher than one assumed from the curvature radius of the apex.

deeply in the cell body) rather than by F-actin mesh (located directly under the plasma membrane). It worth noting that this contradiction is not necessarily a problem because the studied objects were cells of different types. Further research is needed to address this issue.

Now we can conclude that all AFM tips, sharp and colloidal probes, are capable of distinguishing the rigidity of the deep cell body. Secondly, even a sharp AFM probe is capable of detecting the rigidity of cortical cell layer for *some* types of cells. Whereas, to detect alteration in the rigidity in the membrane cell layer for other types of cells, one will presumably need to use a duller, colloidal probe. More generally, future research has to be done. The ability to detect the glycocalyx layer is not clear at the present time for either probes.

### 3.5.2. Biochemical Reasons for the Observed Differences

Oncogenically transformed cells are expected to have differences in all cell layers: the glycocalyx, the cell membrane, and the deep cell body. It is plausible to expect corresponding mechanical alterations in malignant cells. While it is not clear if the layer of glycocalyx can be detected by the AFM method at all, the change in rigidity is expected to come from alterations in the cytoskeleton and of the cell membrane. There have been reports of increased rigidity of tumor cell membranes due to the large increase in their cholesterol content [166]. However, it is unlikely that the membrane can contribute noticeably to AFM force curves, because the membrane is very thin. Nevertheless, direct experiments either proving or disproving this have to be done in the future. So far, the most plausible reason for the observed difference between cancer and normal cells is the alteration in the cytoskeleton. Cancerous transformation is known [167] to accompany morphological alterations in the cytoskeleton. This should lead to changes in cell mechanical properties [168–170]. A simple immunofluorescent experiment can show the difference. Figure 8 shows fluorescent images of human cervical cells, both normal and cancerous. Alexa Fluor 488 phalloidin dye was used to label F-actin for fluorescent imaging (the method is described in Sokolov et al. [171]). One can clearly see the difference in distribution of F-actin. Cancer cells show well-known large nuclei, visible as dark zones in the middle of the tumor cells. Similar measurements [168, 169] done on fibroblasts cells show almost a 50% decrease of F-actin in cancerous cells versus normal ones. Such a decrease is typically explained by the

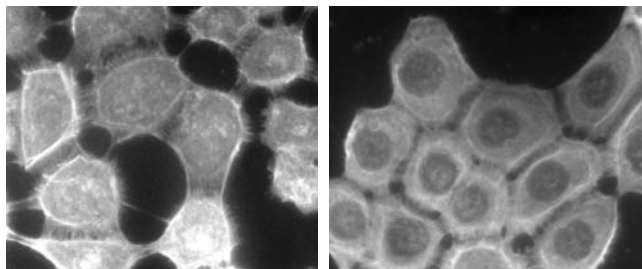


**Figure 8.** Fluorescent images of human cervical cells: (left) normal and (right) cancer. F-actin is labeled with Alexa Fluor 488 phalloidin dye.

faster rate of mitosis of cancer cells, which consequently do not have enough time to develop a cytoskeleton as dense as that in normal cells. Theoretical calculations [169] show that cell rigidity can change by an order of magnitude depending on concentration and the degree of crosslinking of the actin filaments, and their spatial distribution.

Studies using sharp AFM tips reported increasing differences between the Young's modulus of cancer versus that of normal cells, as probe penetration increases. At the present time this can be explained by three separate and possibly interacting reasons. We might be dealing with re-arrangement of F-actin deep inside the cell body. We might be detecting malignant alteration of tubulin. (It may also be that both are true.) The last possible reason is connected with the fact that these results have been reported for the sharp tips; therefore, we might be dealing with a nonlinear response of stretching of the cortical layer. Similar experiments have to be repeated with the colloidal probe tips to help us further elucidate an answer to the problem.

To summarize, a lesser developed cytoskeleton is a clear biochemical reason for the observed decrease in the rigidity of cancer cells. The exact value and nature of such a decrease depends obviously on the type of the cell, type of the cancer, and perhaps other factors which are still unknown.

### 3.5.3. Possible Sources of Uncertainty in the Study of Cell Mechanics

From the previous discussion it is clear that AFM study of cell mechanics and its malignant alteration is in its initial stages. There are many uncertainties that can influence comparison of mechanics of normal and cancer cells. Below we summarize what we have already partially mentioned above. The sources with uncertainties can be classified into categories: preparation of cell culture, and AFM-related issues. They are as follows:

Cell culture uncertainties:

- *Used medium.* Some components of medium can potentially influence rigidity. For example any addition of calcium could trigger a whole series of cell differentiations. Some components of the medium are too difficult to reproduce. For example, serum is too complex a component to be sure that one is getting the same serum every time, or is comparable to what is used by other researchers. At the same time serum can influence cell growth [172]. Serum-free medium would be a better choice, keratinocyte serum free medium, for example.
- *Cell age.* Age of normal cells can cause variations in rigidity by an order of magnitude [133]. One may expect similar behavior for cancerous cells.
- *Mitosis stage.* Cells in different stages of mitosis [141] can have differences in rigidity that vary by an order of magnitude.
- *Confluence of cell culture.* After reaching the confluent stage in the Petri dish, normal cells start to slow down their growth and differentiate, whereas cancer cells keep growing. When comparing cells, one should note the stage of the cell culture in the Petri dish. Unless this is carefully taken into account, different

rates in growth of cancer and normal cells can lead to a different time of exposure of cells to the growth medium, which can potentially influence cell mechanics (see the first uncertainty).

AFM-related uncertainties:

- *Spring constant and tip radius.* Tip radius and spring constant of the cantilever are determined with a finite error.
- *Non-linearity due to AFM tip pressure.* A sharp AFM tip can cause too high a local strain on the cell. This can result in non-linear case of the cell material. The use of dull or modified tips can help to avoid it.
- *Viscoelastic effects.* Because we compare the (quasi) static Young's modulus, there is some error due to the nonzero speed of vertical motion of the probe. One should try to either decrease the speed, or record and report the speed that was used.
- *Heterogeneity of the cell surface.* Some areas on the cell surface may be substantially different from others [133]. If such heterogeneity is observed, an appropriate amount of data has to be collected to get robust statistics. Sometimes when the heterogeneity can be associated with specific areas on the cell surface, it makes sense to compare cancer and normal cells, for each of those areas in turn.
- *Variability of cells.* Due to the intrinsic variability of cells (being biological objects), one should collect enough data to ensure robust statistics via measurements taken on a large number of cells.
- *Non-flat cell geometry.* Simple models typically assume a probe of a known geometry over a flat surface. Therefore, one has to be careful to collect force curves from relatively flat areas of cells. Otherwise, more complicated models have to be used to recover the Young's moduli.
- *Definition of the tip-cell contact.* The difficulty in precise definition of the moment when the AFM probe touches the cell surface is one of the most serious sources of variability of calculated Young's moduli. It is therefore recommended to include this value as an unknown parameter during the model fitting of the force curves, not just graphically.
- *Complexity of cell structure.* It is quite surprising itself that such a complicated system as a biological cell can be described with Young's modulus, which is a characteristic of a simple elastic medium. Clearly, it is an approximation when used with cells. More complicated models [162–164], in which cells are treated at least as a layered material, need to be broadly used in any future research.
- *Poisson ratio.* For the “apparent Young's modulus” that we are describing in this paper, the Poisson ratio is not important. However, it is still very interesting from a fundamental point of view to compare the actual Young's moduli, which *can* be influenced by the Poisson ratio. This will have to be elucidated in future research.
- *Tip-cell adhesion.* Typically the adhesion between the AFM probe and the cell surface is negligible. For some types of probe material, it can nevertheless be large, and can also bring some uncertainty to the definition

of Young's modulus. This therefore must be monitored, and the appropriate JKR model must be used.

The above is a short list of possible factors that can lead to uncertainty in the definition of Young's modulus of the cell. Most assuredly, one can expect that there will be other factors that are not apparent to us at the moment.

## 4. CONCLUSIONS AND FUTURE DIRECTIONS

Atomic force microscopy is clearly a unique tool to provide new information about cells in cancer research. Being a highly sensitive tool, AFM is capable of detecting interactions between single molecules on the AFM tip and those on surfaces of interest. It can detect morphological and mechanical changes at the very early stages. A comparison of the mechanics of normal and tumor cells can reveal new information about, and mechanisms of, malignant transformation. It will also help to understand how cells “mechanically” invade normal tissue. At the present time, there are only a few studies that have been done in this direction. However, even that has already shown the potential to distinguish cancer cells. There is a lot that has to be done. The AFM is known to be able to detect molecular layers. Therefore, AFM is expected to be able to measure the difference in molecular mechanics starting from the layer of glycocalyx. This has not been shown for the case of either cancer or normal cells so far. It is of great interest to understand the contribution of different organelles to cellular mechanics. This may bring new information about the difference between normal and cancer cells. In general, we envision the following developments in research in the nearest future:

- Comparative mechanics of normal versus cancer cells of the same cell type will be done with a sufficient amount of statistical data. This needs to be done with colloidal probes that have a well-defined geometry.
- Study of the influence of malignant transformations on the surface layer of the glycocalyx. This layer is expected to be evident and evaluable in the force curves.
- Finding all factors that can influence rigidity of cells. Many of those potential factors are listed in the previous section.
- Viscoelastic response of the cells depends on the frequency of the oscillating tip. Consequently it carries much more information about cell mechanics than do static experiments. It is not an easy task because it is rather time-consuming to collect enough data to provide robust statistics.
- Cell mechanics tomography. Cells show a clear dependence of rigidity on the depth of probe penetration. It will be interesting to recover a three-dimensional distribution of the Young's modulus from such data. This will be a non-trivial calculation.
- Further development of AFM technique will bring new information. For example, a combination of AFM and fluorescent confocal microscopy is of great interest because it will allow the study of the mechanics of single organelles. A combination of AFM and Raman

confocal microscopy would allow connecting mechanical studies with information about molecular changes in cells.

## ACKNOWLEDGMENTS

The author is thankful to Craig Woodworth for very fruitful and stimulating discussions. I would also like to acknowledge my students and postdoctoral fellows who contributed to many papers cited in this review; in particular, Swaminathan Iyer, Venkatesh Subba-Rao, Tamara Berdyeva, and Yaroslav Kievsky. Partial financial support from NYS-TAR (CAMP-37533391) and NSF (CCF-0304143) are also acknowledged.

## REFERENCES

1. J. L. Alonso and W. H. Goldmann, *Life Sciences* 72, 2553 (2003).
2. H. Arzate, M. A. Alvarez-Perez, M. E. Aguilar-Mendoza, and O. Alvarez-Fregoso, *J. Periodontal Res.* 33, 249 (1998).
3. S. Barakat, L. Gayet, G. Dayan, S. Labialle, A. Lazar, V. Oleinikov, A. W. Coleman, and L. G. Baggetto, *Biochem. J.* 388, 563 (2005).
4. N. P. Barrera, P. Herbert, R. M. Henderson, I. L. Martin, and J. M. Edwardson, *Proc. Natl. Acad. Sci. USA* 102, 12595 (2005).
5. G. Bischoff, A. Bernstein, D. Wohlrab, and H. J. Hein, *Methods Mol. Biol.* 242, 105 (2004).
6. R. Bischoff, G. Bischoff, and S. Hoffmann, *Ann. Biomed. Eng.* 29, 1092 (2001).
7. F. Braet, D. Vermijlen, V. Bossuyt, R. De Zanger, and E. Wisse, *Ultramicroscopy* 89, 265 (2001).
8. C. Brus, E. Kleemann, A. Aigner, F. Czubayko, and T. Kissel, *J. Control. Release* 95, 119 (2004).
9. I. Chasiotis, H. L. Fillmore, and G. T. Gillies, *Nanotechnology* 14, 557 (2003).
10. B. Chen, Q. Wang, and L. Han, *Scanning* 26, 162 (2004).
11. J. Domke, S. Dannohl, W. J. Parak, O. Muller, W. K. Aicher, and M. Radmacher, *Colloids Surf. B Biointerfaces* 19, 367 (2000).
12. A. Drochon, D. Barthes-Biesel, C. Lacombe, and J. C. Lelievre, *J. Biomech. Eng.* 112, 241 (1990).
13. R. H. Eibl and V. T. Moy, *Methods Mol. Biol.* 305, 439 (2005).
14. S. Feng and G. Huang, *J. Control. Release* 71, 53 (2001).
15. S. S. Feng, L. Mu, K. Y. Win, and G. Huang, *Curr. Med. Chem.* 11, 413 (2004).
16. H. L. Fillmore, I. Chasiotis, S. W. Chow, and G. T. Gillies, *Nanotechnology* 14, 73 (2003).
17. C. Fonseca, J. N. Moreira, C. J. Ciudad, M. C. Pedrosa de Lima, and S. Simoes, *Eur. J. Pharm. Biopharm.* 59, 359 (2005).
18. C. Gliss, O. Randel, H. Casalta, E. Sackmann, R. Zorn, and T. Bayerl, *Biophys. J.* 77, 331 (1999).
19. W. H. Goldmann and R. M. Ezzell, *Experimental Cell Research* 226, 234 (1996).
20. W. H. Goldmann, R. Galneder, M. Ludwig, W. M. Xu, E. D. Adamson, N. Wang, and R. M. Ezzell, *Experimental Cell Research* 239, 235 (1998).
21. A. Hategan, R. Law, S. Kahn, and D. E. Discher, *Biophys. J.* 85, 2746 (2003).
22. M. Horton, G. Charras, and P. Lehenkari, *J. Recept Signal Transduct. Res.* 22, 169 (2002).
23. S. Huang and D. E. Ingber, *Cancer Cell* 8, 175 (2005).
24. S. Kusick, H. Bertram, H. Oberleithner, and T. Ludwig, *J. Cell Physiol.* 204, 767 (2005).
25. P. P. Lehenkari, G. T. Charras, S. A. Nesbitt, and M. A. Horton, *Expert. Rev. Mol. Med.* 2000, 1 (2000).
26. M. Lekka, P. Laidler, J. Dulinska, M. Labedz, and G. Pyka, *Eur. Biophys. J.* 33, 644 (2004).
27. M. Lekka, P. Laidler, D. Gil, J. Lekki, Z. Stachura, and A. Z. Hryniewicz, *Eur. Biophys. J. Biophys. Lett.* 28, 312 (1999).
28. M. Lekka, P. Laidler, J. Ignacak, M. Labedz, J. Lekki, H. Struszczyk, Z. Stachura, and A. Z. Hryniewicz, *Biochim. Biophys. Acta.* 1540, 127 (2001).
29. M. Lekka, J. Lekki, M. Marszałek, P. Golonka, Z. Stachura, B. Cleff, and A. Z. Hryniewicz, *Appl. Surf. Sci.* 141, 345 (1999).
30. H. F. Liang, T. F. Yang, C. T. Huang, M. C. Chen, and H. W. Sung, *J. Control. Release* 105, 213 (2005).
31. R. E. Mahaffy, S. Park, E. Gerde, J. Kas, and C. K. Shih, *Biophys. J.* 86, 1777 (2004).
32. R. E. Mahaffy, C. K. Shih, F. C. MacKintosh, and J. Kas, *Phys. Rev. Lett.* 85, 880 (2000).
33. L. Mu and S. S. Feng, *J. Control Release* 86, 33 (2003).
34. H. Muramatsu, N. Chiba, K. Nakajima, T. Ataka, M. Fujihira, J. Hitomi, and T. Ushiki, *Scanning Microsc.* 10, 975 (1996).
35. D. M. Noll, M. Webba da Silva, A. M. Noronha, C. J. Wilds, O. M. Colvin, M. P. Gamcsik, and P. S. Miller, *Biochemistry* 44, 6764 (2005).
36. M. J. Paszek, N. Zahir, K. R. Johnson, J. N. Lakins, G. I. Rozenberg, A. Gefen, C. A. Reinhart-King, S. S. Margulies, M. Dembo, D. Boettiger, D. A. Hammer, and V. M. Weaver, *Cancer Cell* 8, 241 (2005).
37. A. E. Pelling, S. Sehati, E. B. Gralla, J. S. Valentine, and J. K. Gimzewski, *Science* 305, 1147 (2004).
38. K. Poole and D. Muller, *Br. J. Cancer* 92, 1499 (2005).
39. Y. Rabinovich, M. Esayanur, S. Daosukho, K. Byer, H. El-Shall, and S. Khan, *J. Colloid Interf. Sci.* 285, 125 (2005).
40. M. Radmacher, *IEEE Eng. Med. Biol. Mag.* 16, 47 (1997).
41. M. Radmacher, *Methods Cell Biol.* 68, 67 (2002).
42. E. Sackmann, *FEBS Lett.* 346, 3 (1994).
43. G. Sagvolden, I. Giaever, E. O. Pettersen, and J. Feder, *Proc. Natl. Acad. Sci. USA* 96, 471 (1999).
44. S. Sen, S. Subramanian, and D. E. Discher, *Biophys. J.* 89, 3203 (2005).
45. R. Simon, E. Wallraff, J. Faix, J. Niewohner, G. Gerisch, and E. Sackmann, *Biophys. J.* 74, 514 (1998).
46. H. Strey, M. Peterson, and E. Sackmann, *Biophys. J.* 69, 478 (1995).
47. K. Svoboda, C. F. Schmidt, D. Branton, and S. M. Block, *Biophys. J.* 63, 784 (1992).
48. B. Szabo, D. Selmeczi, Z. Kornyei, E. Madarasz, and N. Rozlosnik, *Phys. Rev. E Stat. Nonlin. Soft. Matter. Phys.* 65, 041910 (2002).
49. T. Ushiki, J. Hitomi, T. Umemoto, S. Yamamoto, H. Kanazawa, and M. Shigeno, *Arch. Histol. Cytol.* 62, 47 (1999).
50. G. Binnig, C. F. Quate, and C. Gerber, *Phys. Rev. Lett.* 56, 930 (1986).
51. J. H. Hoh and C. A. Schoenenberger, *J. Cell Sci.* 107, 1105 (1994).
52. I. Y. Sokolov, G. S. Henderson, and F. J. Wicks, *Appl. Surf. Sci.* 140, 362 (1999).
53. F. Ohnesorge and G. Binnig, *Science* 260, 1451 (1993).
54. I. Y. Sokolov, *Appl. Surf. Sci.* 210, 37 (2003).
55. I. Y. Sokolov and G. S. Henderson, *Appl. Surf. Sci.* 157, 302 (2000).
56. S. M. Yang, I. Sokolov, N. Coombs, C. T. Kresge, and G. A. Ozin, *Adv. Mater.* 11, 1427 (1999).
57. D. M. Czajkowsky, H. Iwamoto, and Z. Shao, *J. Electron. Microsc.* (Tokyo) 49, 395 (2000).
58. Y. G. Kuznetsov, A. J. Malkin, and A. McPherson, *J. Struct. Biol.* 120, 180 (1997).
59. D. J. Muller, H. Janovjak, T. Lehto, L. Kuerschner, and K. Anderson, *Prog. Biophys. Mol. Biol.* 79, 1 (2002).
60. Z. Shao, *News Physiol. Sci.* 14, 142 (1999).
61. J. Yang, *Cell Biochem. Biophys.* 41, 435 (2004).
62. J. Zhang, Y. L. Wang, L. Gu, and J. Pan, *Sheng Wu Hua Xue Yu Sheng Wu Wu Li Xue Bao (Shanghai)* 35, 489 (2003).
63. A. Bonfiglio, M. T. Parodi, and G. P. Tonini, *Exp. Cell Res.* 216, 73 (1995).

64. Y. Chen and J. Y. Cai, Sheng Wu Hua Xue Yu Sheng Wu Wu Li Xue Bao (Shanghai) 35, 752 (2003).
65. M. Gorka, W. M. Daniewski, B. Gajkowska, E. Lusakowska, M. M. Godlewski, and T. Motyl, *Anti-Cancer Drugs* 16, 777 (2005).
66. S. Hombach-Klonisch, A. Kehlen, P. A. Fowler, B. Huppertz, J. F. Jugert, G. Bischoff, E. Schluter, J. Buchmann, and T. Klonisch, *J. Mol. Endocrinol.* 34, 517 (2005).
67. M. Malisaukas, J. Ostman, A. Darinskas, V. Zamotin, E. Liutkevicius, E. Lundgren, and L. A. Morozova-Roche, *J. Biol. Chem.* 280, 6269 (2005).
68. K. Matsubara, M. Mizuguchi, K. Igarashi, Y. Shinohara, M. Takeuchi, A. Matsuura, T. Saitoh, Y. Mori, H. Shinoda, and K. Kawano, *Biochemistry* 44, 3280 (2005).
69. H. Ohshiro, R. Suzuki, T. Furuno, and M. Nakanishi, *Immunol. Lett.* 74, 211 (2000).
70. S. Wilkinson, H. F. Paterson, and C. J. Marshall, *Nat. Cell Biol.* 7, 255 (2005).
71. T. K. Berdyeva, C. D. Woodworth, and I. Sokolov, *Phys. Med. Biol.* 50, 81 (2005).
72. A. Ikai, R. Afrin, H. Sekiguchi, T. Okajima, M. T. Alam, and S. Nishida, *Curr. Protein Pept. Sci.* 4, 181 (2003).
73. R. Lal and S. A. John, *Am. J. Physiol.* 266, C1 (1994).
74. E. Lesniewska, M. C. Giocondi, V. Vie, E. Finot, J. P. Goudonnet, and C. Le Grimellec, *Kidney Int. Suppl.* 65, S42 (1998).
75. M. Melling, S. Hochmeister, R. Blumer, K. Schilcher, S. Mostler, M. Behnam, J. Wilde, and D. Karimian-Teherani, *Neuroimage* 14, 1348 (2001).
76. I. Obataya, C. Nakamura, S. Han, N. Nakamura, and J. Miyake, *Biosens. Bioelectron.* 20, 1652 (2005).
77. F. M. Ohnesorge, J. K. Horber, W. Haberle, C. P. Czerny, D. P. Smith, and G. Binnig, *Biophys. J.* 73, 2183 (1997).
78. C. Rotsch and M. Radmacher, *Biophys. J.* 78, 520 (2000).
79. P. Schaefer-Zammaretti and J. Ubbink, *Ultramicroscopy* 97, 199 (2003).
80. H. W. Wu, T. Kuhn, and V. T. Moy, *Scanning* 20, 389 (1998).
81. W. Xu, P. J. Mulhern, B. L. Blackford, M. H. Jericho, M. Firtel, and T. J. Beveridge, *J. Bacteriol.* 178, 3106 (1996).
82. Y. Yamane, H. Shiga, H. Haga, K. Kawabata, K. Abe, and E. Ito, *J. Electron Microsc. (Tokyo)* 49, 463 (2000).
83. L. Zhao, D. Schaefer, and M. R. Marten, *Appl. Environ. Microbiol.* 71, 955 (2005).
84. B. B. Asch, B. R. Kamat, and N. A. Burstein, *Cancer Res.* 41, 2115 (1981).
85. J. Chakraborty and G. A. Von Stein, *Exp. Mol. Pathol.* 44, 235 (1986).
86. R. D. Christen, A. P. Jekunen, J. A. Jones, F. Thiebaut, D. R. Shalinsky, and S. B. Howell, *J. Clin. Invest.* 92, 431 (1993).
87. E. G. Fey and S. Penman, *Dev. Biol. (NY 1985)* 3, 81 (1986).
88. J. D. Han and C. S. Rubin, *J. Biol. Chem.* 271, 29211 (1996).
89. H. Igarashi, H. Sugimura, K. Maruyama, Y. Kitayama, I. Ohta, M. Suzuki, M. Tanaka, Y. Dobashi, and I. Kino, *Apmis* 102, 295 (1994).
90. S. J. Kerr, *Tumour Biol.* 6, 123 (1985).
91. T. Kobayasi, J. Bartosik, and S. Ullman, *J. Dermatol.* 25, 5 (1998).
92. Y. Nishimura, M. Sameni, and B. F. Sloane, *Pathol. Oncol. Res.* 4, 283 (1998).
93. J. Niwa, M. Mori, T. Minase, and K. Hashi, *Exp. Cell Res.* 161, 517 (1985).
94. R. T. Parmley, S. S. Spicer, and A. J. Garvin, *Cancer Res.* 36, 1717 (1976).
95. P. Pippia, L. Sciola, M. A. Meloni, S. Barni, and G. Tilloca, *Boll. Soc. Ital. Biol. Sper.* 65, 453 (1989).
96. N. A. Popoff, *J. Ultrastruct. Res.* 42, 244 (1973).
97. H. Takeshima, T. Nishi, K. Yamamoto, T. Kino, H. Nakamura, H. Saya, M. Kochi, J. I. Kuratsu, and Y. Ushio, *Int. J. Oncol.* 12, 1073 (1998).
98. S. Taniguchi, *Cancer Sci* 96, 738 (2005).
99. I. H. Yang, C. C. Co, and C. C. Ho, *Biomaterials* 26, 6599 (2005).
100. A. Engel and D. J. Muller, *Nat. Struct. Biol.* 7, 715 (2000).
101. D. Fotiadis, S. Scheuring, S. A. Muller, A. Engel, and D. J. Muller, *Micron* 33, 385 (2002).
102. J. H. Hafner, C. L. Cheung, A. T. Woolley, and C. M. Lieber, *Prog. Biophys. Mol. Biol.* 77, 73 (2001).
103. H. G. Hansma, K. Kasuya, and E. Oroudjev, *Curr. Opin. Struct. Biol.* 14, 380 (2004).
104. D. J. Muller, J. B. Heymann, F. Oesterheld, C. Moller, H. Gaub, G. Buldt, and A. Engel, *Biochim. Biophys. Acta.* 1460, 27 (2000).
105. J. P. Xu, J. Ji, W. D. Chen, and J. C. Shen, *Macromol. Biosci.* 5, 164 (2005).
106. biophysics.com (2002).
107. A. Vinckier and G. Semenza, *FEBS Lett.* 430, 12 (1998).
108. D. Cuvelier, I. Derenyi, P. Bassereau, and P. Nassoy, *Biophys. J.* 88, 2714 (2005).
109. F. Gerbal, V. Laurent, A. Ott, M. F. Carlier, P. Chaikin, and J. Prost, *Eur. Biophys. J.* 29, 134 (2000).
110. V. M. Laurent, E. Planus, R. Fodil, and D. Isabey, *Biorheology* 40, 235 (2003).
111. A. R. Bausch, U. Hellerer, M. Essler, M. Aepfelbacher, and E. Sackmann, *Biophys. J.* 80, 2649 (2001).
112. A. R. Bausch, W. Moller, and E. Sackmann, *Biophys. J.* 76, 573 (1999).
113. J. C. Berrios, M. A. Schroeder, and R. D. Hubmayr, *J. Appl. Physiol.* 91, 65 (2001).
114. L. Deng, N. J. Fairbank, D. J. Cole, J. J. Fredberg, and G. N. Maksym, *J. Appl. Physiol.* 99, 634 (2005).
115. W. Feneberg, M. Aepfelbacher, and E. Sackmann, *Biophys. J.* 87, 1338 (2004).
116. V. Heinrich and R. E. Waugh, *Ann. Biomed. Eng.* 24, 595 (1996).
117. H. Huang, R. D. Kamm, P. T. So, and R. T. Lee, *Hypertension* 38, 1158 (2001).
118. G. N. Maksym, B. Fabry, J. P. Butler, D. Navajas, D. J. Tschumperlin, J. D. Laporte, and J. J. Fredberg, *J. Appl. Physiol* 89, 1619 (2000).
119. J. Ohayon and P. Tracqui, *Ann. Biomed. Eng.* 33, 131 (2005).
120. M. Puig-De-Morales, M. Grabulosa, J. Alcaraz, J. Mollo, G. N. Maksym, J. J. Fredberg, and D. Navajas, *J. Appl. Physiol* 91, 1152 (2001).
121. A. Chabanel, D. Schachter, and S. Chien, *Hypertension* 10, 603 (1987).
122. E. A. Evans, R. Waugh, and L. Melnik, *Biophys. J.* 16, 585 (1976).
123. T. C. Havell, D. Hillman, and L. S. Lessin, *Am. J. Hematol.* 4, 9 (1978).
124. O. Linderkamp, E. Friederichs, and H. J. Meiselman, *Pediatr. Res.* 34, 688 (1993).
125. G. B. Nash and W. B. Gratzler, *Biorheology* 30, 397 (1993).
126. G. B. Nash and H. J. Meiselman, *Blood Cells* 17, 517 (1991).
127. M. Paulitschke, J. Mikita, D. Lerche, and W. Meier, *Int. J. Microcirc. Clin. Exp.* 10, 67 (1991).
128. M. Paulitschke, G. B. Nash, D. J. Anstee, M. J. Tanner, and W. B. Gratzler, *Blood* 86, 342 (1995).
129. P. Ulrich and X. Zhang, *Diabetologia* 40, S157 (1997).
130. G. Perry and M. A. Smith, *Free Radical Biology & Medicine* 31, 175 (2001).
131. R. Bucala and A. Cerami, *Advances in Pharmacology* 23, 1 (1992).
132. G. P. Dimri, X. Lee, G. Basile, M. Acosta, G. Scott, C. Roskelley, E. E. Medrano, M. Linskens, I. Rubelj, O. Pereira-Smith, M. Peacocke, and J. Campisi, *Proc. Nat. Acad. Sci. USA* 92, 9363 (1995).
133. T. K. Berdyeva, C. D. Woodworth, and I. Sokolov, *Phys. Med. Biol.* 50, 81 (2005).
134. A. A. L. Weisenhorn, A. M. Khorsandi, A. S. Kasas, A. V. Gotzos, and A. H. J. Butt, *Nanotechnology* 4, 106 (1993).

135. C. A. Bippes, A. D. Humphris, M. Stark, D. J. Muller, and H. Janovjak, *Eur. Biophys. J.* 1 (2005).
136. C. Rotsch, F. Braet, E. Wisse, and M. Radmacher, *Cell Biol. Int.* 21, 685 (1997).
137. H. W. Wu, T. Kuhn, and V. T. Moy, *Scanning* 20, 389 (1998).
138. M. Radmacher, *IEEE Eng. Med. Biol. Mag.* 16, 47 (1997).
139. R. Matzke, K. Jacobson, and M. Radmacher, *Nat. Cell Biol.* 3, 607 (2001).
140. D. Ricci and M. Grattarola, *J. Microsc.* 176, 254 (1994).
141. R. Matzke, K. Jacobson, and M. Radmacher, *Nat. Cell Biol.* 3, 607 (2001).
142. M. Glogauer, P. Arora, G. Yao, I. Sokolov, J. Ferrier, and C. A. McCulloch, *J. Cell Sci.* 110, 11 (1997).
143. E. K. Dimitriadis, F. Horkay, K. Bechara, and R. S. Chadwick, *Biophys. J.* 82, 56A (2002).
144. B. Shoelson, E. K. Dimitriadis, H. X. Cai, B. Kachar, and R. S. Chadwick, *Biophys. J.* 87, 2768 (2004).
145. E. K. Dimitriadis, F. Horkay, B. Kachar, and R. S. Chadwick, *Abstracts of Papers of the American Chemical Society* 224, U417 (2002).
146. E. K. Dimitriadis, F. Horkay, J. Maresca, B. Kachar, and R. S. Chadwick, *Abstracts of Papers of the American Chemical Society* 223, C113 (2002).
147. G. Bogdanovic, A. Meurk, and M. W. Rutland, *Colloids and Surfaces B-Biointerfaces* 19, 397 (2000).
148. P. J. Cumpson, P. Zhdan, and J. Hedley, *Ultramicroscopy* 100, 241 (2004).
149. F. L. Degertekin, B. Hadimioglu, T. Sulchek, and C. F. Quate, *Appl. Phys. Lett.* 78, 1628 (2001).
150. C. T. Gibson, B. L. Weeks, C. Abell, T. Rayment, and S. Myhra, *Ultramicroscopy* 97, 113 (2003).
151. R. Levy and M. Maaloum, *Nanotechnology* 13, 33 (2002).
152. J. E. Sader, I. Larson, P. Mulvaney, and L. R. White, *Rev. Sci. Instrum.* 66, 3789 (1995).
153. T. E. Schaffer, *Nanotechnology* 16, 664 (2005).
154. I. N. Sneddon, *Int. J. Eng. Sci.* 3, 47 (1965).
155. V. V. Tsukruk, V. V. Gorbunov, Z. Huang, and S. A. Chizhik, *Polymer Intern.* 5, 441 (2000).
156. D. H. Gracias and G. A. Somorjai, *Macromolecules* 31, 1269 (1998).
157. C. S. Hodges, J. A. S. Cleaver, M. Ghadiri, R. Jones, and H. M. Pollock, *Langmuir* 18, 5741 (2002).
158. C. S. Hodges, L. Looi, J. A. S. Cleaver, and M. Ghadiri, *Langmuir* 20, 9571 (2004).
159. K. Meine, K. Kloss, T. Schneider, and D. Spaltmann, *Surf. Interface Anal.* 36, 694 (2004).
160. S. Pal and S. Banerjee, *J. Phys. D: Appl. Phys.* 34, 253 (2001).
161. X. P. Yu and A. A. Goldenberg, *Int. J. Nonlinear Sci.* 3, 621 (2002).
162. S. Park, D. Koch, R. Cardenas, J. Kas, and C. K. Shih, *Biophys. J.* doi:10.529/biophysj.104.053462 (2005).
163. Y. O. Tu and D. C. Gazis, *J. Appl. Mech.* 659 (1964).
164. W. T. Chen, *Int. J. Eng. Sci.* 9, 775 (1971).
165. S. Kasas, X. Wang, H. Hirling, R. Marsault, B. Huni, A. Yersin, R. Regazzi, G. Grenningloh, B. Riederer, L. Forro, G. Dietler, and S. Catsicas, *Cell Motil. Cytoskeleton* 62, 124 (2005).
166. M. U. Dianzani, *Tumori* 75, 351 (1989).
167. K. Takahashi, U. I. Heine, J. L. Junker, N. H. Colburn, and J. M. Rice, *Cancer Res.* 46, 5923 (1986).
168. F. Wottawah, S. Schinkinger, B. Lincoln, R. Ananthakrishnan, M. Romeyke, J. Guck, and J. Kas, *Phys. Rev. Lett.* 94, 098103 (2005).
169. J. Guck, S. Schinkinger, B. Lincoln, F. Wottawah, S. Ebert, M. Romeyke, D. Lenz, H. M. Erickson, R. Ananthakrishnan, D. Mitchell, J. Kas, S. Ulvick, and C. Bilby, *Biophys. J.* 88, 3689 (2005).
170. F. C. MacKintosh, J. Kas, and P. A. Janmey, *Phys. Rev. Lett.* 75, 4425 (1995).
171. I. Sokolov, S. Iyer, and C. D. Woodworth, unpublished manuscript submitted to *Nanomedicine* (2006).
172. R. Pfab, D. O. Schachtschabel, N. Paul, H. F. Kern, and F. Hess, *Strahlentherapie* 154, 692 (1978).
173. A. R. Kirby, D. J. Fyfe, M. J. Parker, A. P. Gunning, P. A. Gunning, and V. J. Morris, *Probe Microscopy* 1, 153 (1998).
174. M. Firtel, G. Henderson, and I. Sokolov, *Ultramicroscopy* 101, 105 (2004).